Fatigue Load Conditions

33

Ian A. Ashcroft

Contents

Abstract

Fatigue involves the failure of materials under cyclic loading, where the maximum load can be significantly lower than that required to cause static failure. Polymeric adhesives, as with most materials, are susceptible to fatigue failure, and hence, fatigue should be accounted for when designing bonded structures subjected to cyclic loading. Adhesive joints have potentially good fatigue resistance compared with other joining methods; however, they are also susceptible to accelerated fatigue failure due to the combined actions of fatigue with

I. A. Ashcroft (✉)
Faculty of Engineering, University of Nottingham, Nottingham, UK
e-mail: ian.ashcroft@nottingham.ac.uk

environmental ageing and/or viscoelastic creep. In this chapter, the effect of the environment and various fatigue loading parameters on the fatigue behavior of adhesively bonded joints is discussed before describing the main methods of characterizing and predicting fatigue. Traditionally, fatigue behavior has been characterized through the use of experimentally derived stress–life plots, and fracture mechanics-based progressive crack growth methods have also been widely discussed. In more recent years, damage mechanics-based progressive modeling methods have been proposed that have the advantage of predicting both initiation and crack progression phases of fatigue and have also been shown to be readily adapted to the prediction of variable amplitude fatigue and combined fatigue-environmental ageing. The chapter finishes with descriptions of two special cases of fatigue: creep-fatigue and impact fatigue, which have been shown to be extremely detrimental to the fatigue life of bonded joints under certain conditions.

33.1   Introduction

In engineering, fatigue relates to the failure of a structure under cyclic loading, generally, at a significantly lower load than that required for quasistatic failure. Some form of fatigue loading is present in most engineering structures, for example, aircraft, ships, cars, buildings, and bridges, and is also seen in many nonengineering applications, such as sports equipment, furniture, and even human parts, such as knees and elbows. Fatigue is a particularly dangerous phenomenon as it can result in sudden, catastrophic failure after many years, or decades, of safe service. This is because a long period can be spent in the initiation phase of fatigue damage, in which there are little or no outward signs of damage. Damage can accelerate unstably once a critical degree of damage has been attained, leading to rapid failure of the structure. Fatigue damage can be initiated or accelerated by many factors, such as accidental impact, overloading, corrosion, surface damage, and abrasion.

The ubiquitous nature and potentially disastrous effect of fatigue in engineering structures means that in applications where cyclic loading is significant, the designer must attempt to design against fatigue failure. Unfortunately, the stochastic nature of fatigue damage means it is difficult to predict accurately. This difficulty is compounded by the fact that the in-service loading and environment of many engineering components, which can significantly affect the fatigue process, are seldom known to a great degree of accuracy. Hence, it is generally difficult to design against fatigue failure without resorting to large safety factors, and hence incurring the large structural inefficiencies associated with overdesign, with subsequent cost and performance consequences. An alternative to designing against fatigue failure is to monitor parts for fatigue damage at prescribed intervals and remove them from service before damage reaches a critical point. This is a useful and efficient method of preventing fatigue failure where crack growth is stable and can be easily monitored. However, in some cases, such as is often the case with adhesive joints, monitoring fatigue damage is difficult, for example, if the damage initiation is in an

inaccessible location or the critical crack size before rapid fracture is small. In this case, an alternative strategy is required to combat fatigue, such as automatic replacement of parts after the design life or a "safe fail" design.

One of the benefits of bonded joints is that stresses are more uniformly distributed than in riveted or bolted joints. However, stress concentrations will, of course, still exist in bonded joints, as discussed in detail in ▶ Chaps. 24, "Analytical Approach," and ▶ 25, "Numerical Approach: Finite Element Analysis." Another potential advantage is that the bonding process does not explicitly weaken the adherends as the high temperatures and phase transformations involved in welding and the hole drilling required for rivets and bolts can. Although, it should be noted that there are likely to be stress concentrations in the adherend in the joint area which may initiate adherend fatigue failure, such as is seen in aluminum adherend single-lap joints at high cycles and in the delamination of composite adherends. In general, adhesively bonded joints perform well in fatigue compared with bolted and welded joints; however, a number of potential problems for adhesive joints subjected to fatigue should also be recognized. Both the adhesive and the interfacial region between adhesive and adherend are potentially sensitive to the environment and this will affect the fatigue resistance of the joint. Adhesives can also be susceptible to creep under certain conditions, and combined with fatigue this can lead to accelerated failure. In a bonded joint, failure can occur in the adhesive, in the adherend, or in the interfacial region between the two, and the relative fatigue resistance of the various components is dependent on many factors, such as geometry, environment, and loading, and may vary as damage progresses. This complex failure process means that it can be difficult to accurately predict fatigue failure in adhesively bonded joints under real service conditions.

Section 2 discusses some of the main factors when considering fatigue, with particular reference to issues applicable to bonded joint. Section 3 discusses how various loading parameters and environmental conditions affect the fatigue behavior of bonded joints. Section 4 presents the main methods of characterizing and predicting the response of bonded joints to fatigue loading. Finally, there are sections on the special cases of creep-fatigue and impact fatigue (Sects. 5 and 6), before the final summary and conclusion.

33.2   General Considerations

33.2.1 Fatigue Loading

In fatigue, the load varies with time, and the load spectrum is usually characterized in terms of peaks and troughs in the varying load. A fatigue cycle is defined as the time between adjacent peaks, and the fatigue frequency is the number of cycles in a unit time, for example, Hz (cycles per second). A fatigue spectrum can be characterized in terms of the applied load or displacement for simple samples, but in more complex structures, it is often more useful to consider the cyclic stress (or some other

Fig. 1 Constant amplitude, constant frequency, stress-controlled, sinusoidal waveform
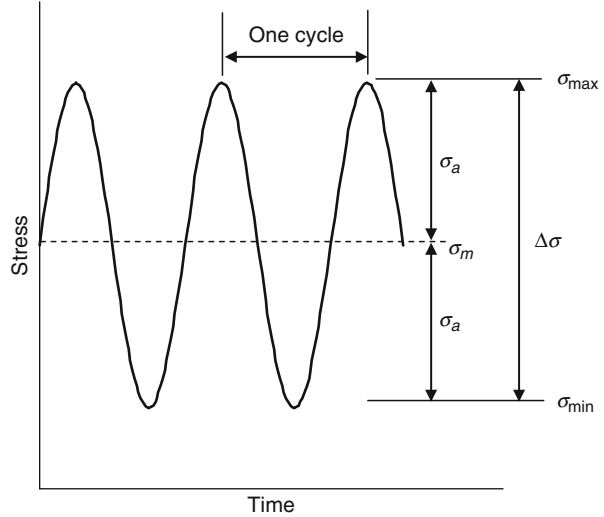

parameter that can be related to failure, such as strain or strain energy release rate) in areas of possible fatigue failure.

It is common in laboratory experiments to represent fatigue as a constant amplitude, sinusoidal waveform, as illustrated in Fig. 1. This is termed constant amplitude fatigue (CAF) and the waveform may be defined by the frequency and two stress parameters, such as the maximum stress (σ_{max}) and the stress amplitude (σ_a). Other parameters defined in Fig. 1 are the mean stress (σ_m), the minimum stress (σ_{min}), and the stress range ($\Delta\sigma$). In most engineering applications, however, it is likely that frequency, amplitude, mean, and waveform will vary with time. This is called variable amplitude fatigue (VAF). The first step in analyzing components subjected to VAF is the characterization of fatigue spectra experienced by the component in service. It is possible to characterize the in-service load spectra through simulation or experimentation. In some cases, a typical spectrum may be repeated throughout the structure's life and will be similar for each structure manufactured, for example, the takeoff and landing sequences of a commercial passenger aircraft or the run-up sequence of power generation equipment. However, for many applications, e.g., private cars, the spectra can vary considerably from unit to unit. In this case, a "worst-case scenario" or statistical approach may have to be taken.

Once the in-service load spectrum has been generated, it can be used in simulations and/or testing. In order to accelerate a fatigue test program, it is generally preferable to reduce the spectrum. In metals, where the materials may be rate insensitive over a large range, an easy method of accelerating tests is to compress the spectrum by testing at high frequency, although any time-dependent effects, such as corrosion or creep, will not be accurately represented in such a test. Hence, when devising accelerated service simulation tests for adhesive joints, care must be taken

Fig. 2 Example of a load-controlled, variable amplitude waveform
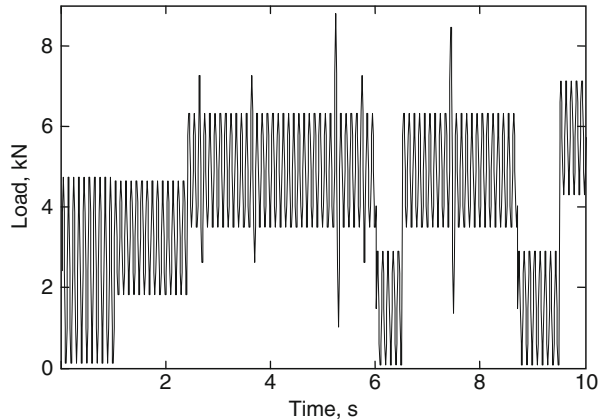
when introducing acceleration techniques that any influential time-dependent or load sequencing effects are retained in the spectrum. Another way of reducing the spectrum is to remove cycles from the spectrum that do not contribute to the fatigue damage. Figure 2 shows a reduced fatigue spectrum used to represent the fatigue loading on an aircraft wing. It can be seen that this is a load-controlled fatigue spectrum that includes changes in the load amplitude and mean, but maintains a constant frequency.

33.2.2 Fatigue Initiation and Propagation

The fatigue life of a structure is often divided into initiation and propagation phases. In adhesively bonded joints, the differentiation between these two phases, and even if there really are two such phases, remains a contentious issue. At the predictive modeling level, a distinction can be made between how a propagating crack is analyzed and how the number of cycles before a macrocrack has formed can be predicted, and this can pragmatically be used to differentiate between the initiation and propagation phases.

Fatigue initiation in adhesives is a complex and little-understood process. Commercial adhesives are multicomponent materials, with filler particles, carrier mats, and toughening particles typically added, and failure may involve many mechanisms, including matrix microcracking (initiation, growth, and coalescence), filler particle fracture or debonding, cavitation of rubber toughening particles, and debonding of carrier mat fibers. An additional difficulty in characterizing the fatigue initiation process in bonded joints is that initial damage tends to be internal. This makes nondestructive characterization difficult, whereas with destructive character-ization methods, it is difficult to avoid sectioning artifacts. In most cases, a purely mechanistic definition of the initiation and propagation phases is not achievable, and a more pragmatic approach must be taken. In terms of in-service inspection,

initiation may be linked to the detectability of flaws, the end of the initiation life being indicated by the first detection of a crack using whatever technique is being deployed. For the stress analyst, a useful differentiation is to treat the fatigue damage as an initiation phase until a sufficient crack has formed that further growth can be predicted using fracture mechanics. In finite element-based damage mechanics, the initiation phase can be defined as the period before complete damage of an element.

Mechanistically, there is also a blurring between the definitions of "damage" and "cracking" in a bonded joint. For example, a region considered as damaged rather than cracked will often contain microcracking, and in a cracked joint, only an idealized version of the main macrocrack is usually considered, whereas this will almost certainly be accompanied by other types of damage in a process zone ahead and around the main crack. In finite element modeling, damage is often represented by reducing the material properties (the continuum damage mechanics approach), usually stiffness, of an element. Cracking is usually modeled by detaching elements at nodes, after which fracture mechanics methods can be used to model crack propagation. In cohesive zone modeling, both damage and crack growth are represented by using specialized elements to join adjacent continuum elements. This is discussed in detail in ▶ Chap. 25, "Numerical Approach: Finite Element Analysis."

33.2.3 Fatigue Testing

Mechanical testing of bonded joints can range from inexpensive coupon tests through the testing of structural elements to the testing of full prototypes, which may be extremely expensive. In all cases, however, fatigue testing will be considerably lengthier and more costly than quasistatic testing.

Coupon tests can fulfil a number of roles. Single material tests may be used to generate material property data, while joints can be tested to compare material systems or joint geometries, evaluate performance over a range of loading and environmental conditions, generate design data, or provide validation data for predictive models. Coupon samples used in the fatigue testing of bonded joints are similar to those used in quasistatic testing, as discussed in ▶ Chaps. 19, "Failure Strength Tests," and ▶ 20, "Fracture Tests." Simple lap joints, such as single- and double-lap joints, are generally used to generate stress–life (S–N) curves, and standard fracture mechanics tests, such as the double cantilever beam, are used to generate fatigue crack growth curves. The fatigue testing of adhesive lap joints is covered by the standards BS EN ISO 9664:1995 and ASTM D3166-99. In the former, it recommends that at least four samples should be tested at three different stress amplitude values for a given stress mean, such that failure occurs between 10^4 and 10^6 cycles. This standard also advises on statistical analysis of the data. In general, fatigue data exhibits greater scatter than quasistatic data and this needs to be taken into account when using safety factors with fatigue data. Further advice on the application of statistics to fatigue data can be found in BS 3518-5:1966.

33.3   Factors Affecting Fatigue Behavior

33.3.1 Load Factors

Load factors that will affect the fatigue behavior of adhesively bonded joints include the amplitude, mean, and minimum stresses and frequency. In common with most materials, fatigue life in a bonded joint will tend to decrease if the stress amplitude or the mean stress increases. The maximum stress is also important. If this is greater than the yield stress, then low cycle fatigue (LCF) will occur, greatly reducing the fatigue life. In some cases, a critical stress, called an endurance limit, may exist, below which fatigue failure will not occur. As adhesives tend to be viscoelastic or viscoplastic in nature, then a nonzero mean stress can lead to progressive creep of the joint over time. This is exacerbated at low frequencies, where time under load may become as significant as number of cycles in defining failure. At high frequencies, hysteretic heating may lead to premature failure or the high strain rates involved may induce brittle fracture. High strain rates are also seen in impact fatigue, in addition to dynamic effects, which, as discussed in Sect. 6, can be extremely detrimental to adhesives. Most bonded joints are designed for tensile loading, and if the joint is subjected to accidental compressive loading, then buckling may occur, from which high peel forces will arise, leading to rapid fracture.

In variable amplitude fatigue, load interaction effects have been observed to both accelerate and retard the rate of fatigue damage, in different materials. Fatigue crack growth rate retardation is probably the more commonly reported phenomenon. For example, it is generally reported that overloads retard fatigue crack propagation in ductile metals. Proposed mechanisms to account for this phenomenon include the effect of compressive residual stresses in the vicinity of the crack tip, crack tip closure effects, and crack tip blunting. Although neglecting such beneficial effects by using a noninteractive lifetime predictive methodology can remove the opportunity to achieve a lighter structure, at least, the design errs on the side of safety. However, if the load interactions cause crack growth acceleration, the structure under investigation can fail much earlier than predicted using CAF data and a noninteractive prediction methodology. Although most published work indicates retardation behavior after an overload, there is also work in the literature reporting crack growth acceleration for both metals and composites. These studies report several different mechanisms accounting for the acceleration behavior. For example, Nisitani and Nakamura (1982) studied the crack growth behavior of steel specimens tested under a spectrum composed of a very small number of overloads and a very large number of cycles below or near the fatigue limit. They observed that the application of a linear cumulative damage rule resulted in extremely nonconservative predictions of fatigue life. A possible explanation was that although understress cycles cannot initiate a crack, they can potentially contribute to the fatigue damage created by overloads. Farrow (1989) found that the fatigue life of composite laminates subjected to small block loading was shorter than that for laminates subjected to large block loadings when the blocks had different mean stress levels. He called this phenomenon the "cycle mix effect." Schaff and

Davidson (1997a, b) reviewed the study made by Farrow and developed a strength-based wearout model. They suggested that the cycle mix effect occurred during the transition from one CAF stage to another having a higher mean stress value, although they did not discuss the mechanisms behind the strength degradation during this transition. Erpolat et al. (2004a) observed a similar crack acceleration effect when VAF testing bonded CFRP double-lap joints.

33.3.2 Environmental Factors

It is well known that adhesives and adhesion can be adversely affected by factors in the natural environment effects, and that this is a topic of considerable complexity (see ▶ Chap. 31, "Effect of Water and Mechanical Stress on Durability"). When environmental effects are combined with fatigue testing, we have an added complexity, owing to the introduction of coupled time-dependent effects. The main effects of environmental exposure can be classified as those affecting the adhesive, those affecting the adherend, and those affecting the interface (or interphase) between the two. In terms of the adhesive, an increase in temperature or the absorption of moisture generally results in plasticization of the adhesive, with an accompanying reduction in modulus and failure load. However, strain to failure and fracture toughness may increase. This can affect fatigue initiation and propagation in a number of ways. The plasticization will tend to reduce stress concentrations, although stresses may now be significant over a larger area; hence, the resistance to brittle fatigue failure may increase, but the resistance to creep-fatigue may decrease. These effects will become more significant close to the glass transition temperature (T_g), and similarity can be seen between the effects of absorbed moisture, increased temperature, and decreased test rate (or frequency). Some of these issues are illustrated by the results shown in Table 1 (data from Ashcroft et al. 2001a, b). This table shows the fatigue limits for bonded CFRP lap-strap and double-lap joints. In the case of the lap-strap joints, it can be seen that temperature has little effect on

Table 1 Effect of environment on the fatigue limit for bonded CFRP-epoxy lap-strap and double-lap joints (Data from Ashcroft et al. 2001a, b)

Sample	Preconditioning	Test conditions	Fatigue limit (kN)
Lap-strap joint	Vacuum desiccator	−50 °C/ambient	14
		22 °C/ambient	15
		90 °C/ambient	14
		90 °C/97% RH	7
	45 °C/85% RH	22 °C/95% RH	15
		90 °C/ambient	5
		90 °C/97% RH	5
Double-lap joint	Vacuum desiccator	−50 °C/ambient	10
		22 °C/ambient	10
		90 °C/ambient	3.3

the fatigue threshold of those sample stored and tested in nominally dry conditions. However, samples tested in hot-wet conditions experience a significant reduction in the fatigue threshold. Samples were also conditioned under high humidity conditions until saturation. Samples subsequently tested wet at 22 °C had no change in the fatigue threshold compared to those tested dry, whereas samples tested at 90 °C, whether wet or dry, experienced a large reduction in the fatigue threshold. Interpretation of these results is complicated by the fact that complex mixed mode failure paths were observed. In order to explain these results, the effect of temperature and moisture on the mechanical behavior of the adhesive must be considered. The stress to failure and modulus of the adhesive decreases as the temperature increases, but the strain to failure and total strain energy density at failure increases. The competing effects of these different trends conspire to maintain the fatigue limit at a relatively constant value between 22 °C and 90 °C when stored and tested dry. Differential thermomechanical analysis (DTMA) was carried out on samples saturated to different moisture levels, and it was seen that for every 1% of moisture absorbed, the glass transition point of the adhesive decreased by approximately 15 °C. As the T_g of this adhesive is approximately 130 °C, the saturated adhesive tested at 22 °C would not be expected to behave markedly differently from those tested dry at 22 °C and 90 °C. However, the saturated sample tested at 90 °C is in the glass transition temperature range as the adhesive is capable of absorbing 3–4% of moisture. It is clearly less capable of resisting stress under these conditions, and hence the fatigue limit is greatly reduced. If the lap-strap results are now compared with the results from testing double-lap joint manufactured using the same materials, it can be seen in Table 1 that whereas the lap-strap joints are relatively temperature insensitive over the test range when dry, the double-lap joints experience a large decrease in fatigue resistance as temperature is increased from 22 °C to 90 °C. This can be attributed to creep-enhanced failure at the higher temperature in the double-lap joint, which experiences accumulated creep because the joint remains under a tensile load throughout the fatigue testing. This phenomenon is prevented in the case of the lap-strap joints because the CFRP strap adherend spanning the loading points remains elastic. The combined effects of fatigue and creep are discussed further in Sect. 5.

Moisture can also affect the interface between the adhesive and adherend, and this can significantly affect the fatigue behavior of a bonded joint. For example, Little (1999) carried out fatigue tests on aluminum single-lap joints bonded with the same adhesive as that in the experiments discussed above. He found that with chromic acid-etched (CAE) adherends, there was little difference in the fatigue threshold of those samples tested dry and those tested immersed in distilled water at 28 °C. However, samples with grit-blasted and degreased (GBD) adherends exhibited a significantly lower fatigue threshold when tested wet, and the locus of failure changed from cohesive failure in the adhesive to failure in the interfacial region. Datla et al. (2011a) also investigated the combined effects of temperature and humidity on the fatigue behavior of adhesive joints with pretreated aluminum adherends. In their case, an asymmetric double cantilever beam was used and it was found that for their system, the joint degradation was mainly influenced by

elevated temperature at high crack growth rates and elevated moisture at low crack growth rates. They also investigated the effect of a cyclic ageing environment for this joint, with intermittent salt spray on these joints (Datla et al. 2011b) and found superior fatigue performance compared with joints subjected to constant humidity ageing. They attributed this to salt water environment causing lower water concentrations in the adhesive. For further reading on this subject, Costa et al. (2017) have recently reviewed the published literature regarding the effect of environmental conditions and ageing on fatigue performance.

33.4   Prediction Methods

The ability to predict the fatigue behavior of bonded joints is potentially useful for a number of reasons. Firstly, it can be used to support the design of bonded structures, to ensure that fatigue failure is not likely to occur in service, and to aid in the design of efficient fatigue-resistant joints, resulting in safer, cheaper, and higher performance structures. Analytical or computational predictive modeling can help in these objectives; however, the current state of confidence in such modeling means that in most cases, it must be accompanied by a complementary testing program. Modeling can also be helpful in developing and understanding of the mechanisms involved in fatigue failure. This can be achieved through comparing the results from carefully designed experimental tests with the predicted results from progressive damage models. Finally, predictive modeling can be used to support the in-service monitoring and re-lifeing of structures.

The main goals in the modeling of fatigue are to predict the time (or number of cycles) for a certain event to occur (such as macrocrack formation, critical extent of damage, or complete failure) or to predict the rate of change of a fatigue-related parameter, such as crack length or "damage." The various methods of doing this are presented in this section, and the approach used is to introduce and describe each of the main methods that have been used to date, together with one or two examples of their application to bonded joints.

33.4.1 Total-Life Methods

In the total-life approach, the number of cycles to failure (N_f) is plotted as a function of a load-related variable, such as stress or strain amplitude. Where the loading is low enough that the deformation is predominantly elastic, a stress variable (S) is usually chosen and the resultant plot is termed an S–N curve, or Wöhler plot, and this is known as the stress–life approach. Under these conditions, a long fatigue life is often seen, and hence this is sometimes termed "high cycle fatigue" (HCF). The S–N data is either plotted as a log-linear or a log-log plot and a characteristic equation can be obtained by empirical curve fitting. The constants in the curve-fitted equations are dependent on many factors, including material, geometry, surface condition, environment, and mean stress. Caution should be exercised when trying to apply S–N
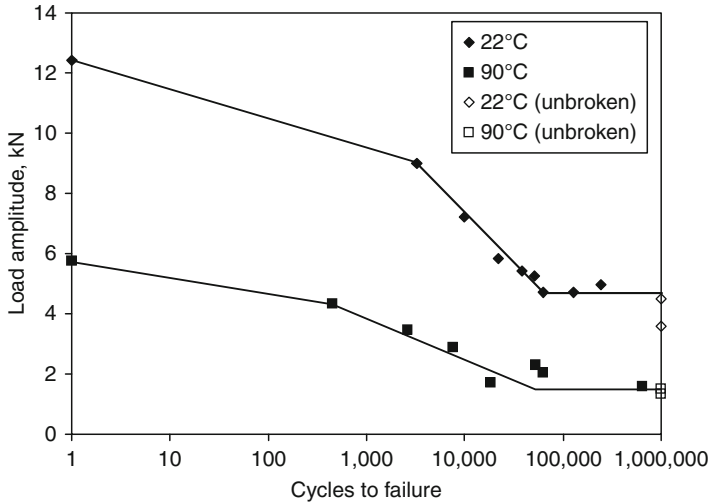
Fig. 3 Load–life curve for CFRP-epoxy double-lap joints (Data from Ashcroft et al. 2001b)

data beyond the samples and conditions used to generate the data. The standard stress–life method gives no indication of the progression of damage, although in some cases, the onset of cracking is indicated on the plot in addition to the complete failure, hence allowing the initiation and propagation phases to be differentiated. The above factors mean that the S–N curve is of rather limited use in predicting fatigue behavior; however, it is still useful as a design tool and in fatigue modeling as a source of validation data. A further limitation in the application of S–N curves to fatigue prediction in bonded joints is that there is no unique relation between the easily determined average shear stress in the adhesive layer and the maximum stress. For this reason, load rather than stress is often used in total-life plots for bonded joints and these are known as L–N curves. A typical L–N curve for epoxy-bonded CFRP double-lap joints is shown in Fig. 3. It can be seen that the L–N curve can be divided into a number of different regions: a low cycle fatigue (LCF) region below approximately 1000 cycles, a high cycle fatigue (HCF) region between approximately 1000 and 100,000 cycles, and an endurance limit region above approximately 100,000 cycles.

Fatigue life depends not only on the load amplitude but also on the mean load as either increasing the mean or increasing the amplitude tends to result in a reduction of the fatigue life. This is illustrated in Fig. 4a, which shows results from fatigue testing steel-epoxy single-lap joints at different load amplitudes and R-ratios (maximum load/minimum load), where an increasing value of R indicates an increasing mean for a given load range. It can be seen that either increasing the mean or increasing the amplitude results in a reduction of the fatigue life. The relationship between amplitude and mean on the fatigue life can be illustrated in a constant-life diagram in which combinations of mean and amplitude are plotted for a given fatigue life. A constant-life diagram plotted from the data in Fig. 4a is shown in Fig. 4b. This
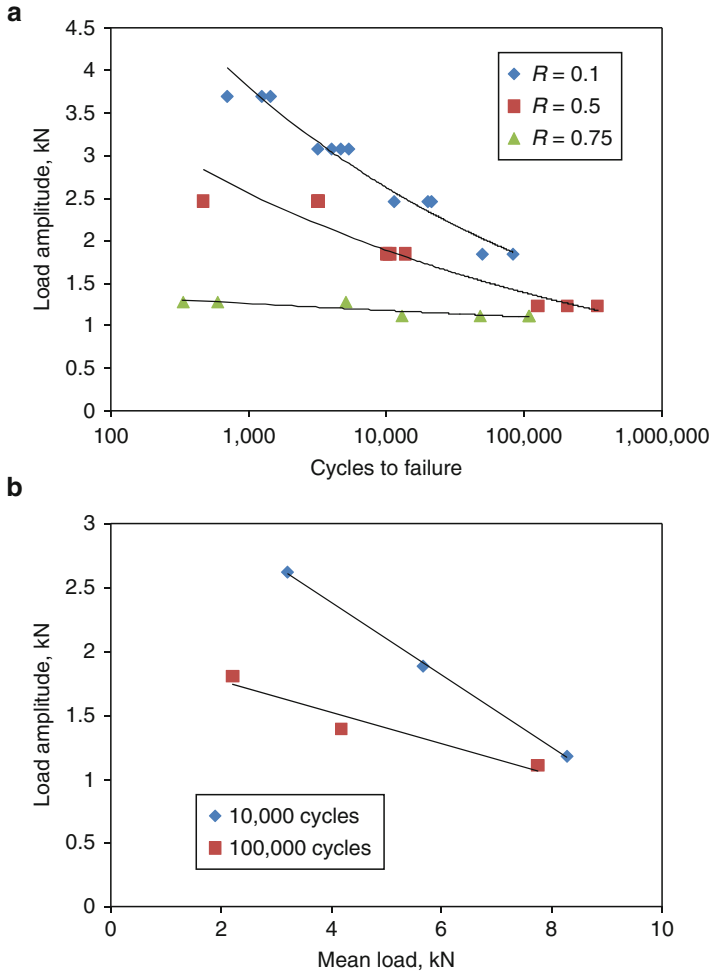
Fig. 4 (**a**) Effect of *R*-ratio on fatigue life. (**b**) Constant-life diagram (Data from Crocombe and Richardson 1999)

relationship can be represented by the Goodman (linear) or Gerber (parabolic) relationships (Dowling 1999). It can be seen that in this case, a linear relationship provides a reasonable fit to the experimental data.

In some cases, efforts have been made to differentiate between the initiation and propagation phases in the *S–N* behavior of bonded joints. Shenoy et al. (2009a) used a combination of back-face strain measurements and sectioning of partially fatigued joints to measure damage and crack growth as a function of number of fatigue cycles.

It was seen from the sectioned joints that there could be extensive internal damage in the joint without external signs of cracking; therefore, determination of an initiation phase from external observations alone is likely to lead to an

Fig. 5 Enhanced load–life curve for adhesively bonded single-lap joints, showing regions of crack initiation (CI), stable crack growth (SCG), and fast crack growth (FG). The broken lines show back-face strain as a function of number of cycles (Shenoy et al. 2009a)
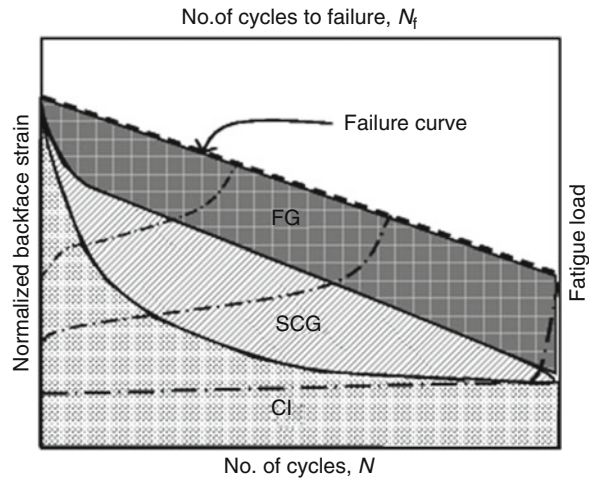

overestimation of the percentage of the fatigue life sent in initiation. Shenoy et al. (2009a) identified three regions in the fatigue life of an aluminum/epoxy single-lap joint, as illustrated in Fig. 5. An initiation period (CI) in which damage starts to accumulate, but a macrocrack has not yet formed, a stable crack growth (SCG) region in which a macrocrack has formed and is growing slowly, and a fast crack growth region (FCG), which leads to rapid failure of the joint. It was seen that the percentage of life spent in each region varied with the fatigue load. At low loads, the fatigue life was dominated by crack initiation, whereas crack growth dominated at high loads. The broken lines in Fig. 5 show how the back-face strain signal varies as a function of fatigue cycles. This can be used to characterize the different phases of crack growth, in particular a rapid change in the back-face strain is seen when the fatigue failure enters the fast crack growth region.

The S–N (or L–N) curve is only directly applicable to constant amplitude fatigue, whereas in most practical applications for structural joints a variable amplitude fatigue spectrum is more likely. A simple method of using S–N data to predict variable amplitude fatigue is that proposed by Palmgren (1924) and further developed by Miner (1945). The Palmgren–Miner (P–M) rule can be represented by

$$\sum \frac{n_i}{N_{fi}} = C \qquad (1)$$

where n_i is the number of cycles in a constant amplitude block, N_{fi} is the number of cycles to failure at the stress amplitude for that particular block and can be obtained from the S–N curve, and C is the Miner's sum and is ideally assumed to equal 1. Using Eq. (1), the fatigue life of a sample in variable amplitude fatigue can be predicted from an S–N curve obtained from constant amplitude fatigue testing of similar samples. However, there are a number of serious limitations to this method, primarily, the assumptions that damage accumulation is linear, that there is no damage below the fatigue threshold, and that there are no load history effects.

Fig. 6 Comparison of P–M, extended P–M, and elementary P–M methods of predicting variable amplitude fatigue cycles to failure
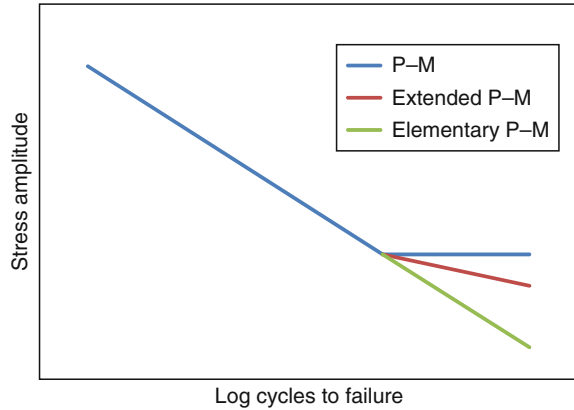
Modifications to the P–M rule have been suggested to address some of the deficiencies; for instance, the extended and elementary P–M rules shown in Fig. 6 have been proposed to allow cycles below the fatigue threshold to contribute to the damage sum. Modifications to account for nonlinear damage accumulation and interaction effects have also been suggested; however, any improvements are at the expense of increased complexity and/or increased testing requirements, and the basic flaw in the method, i.e., that it bears no relation to the actual progression of damage in the sample, is still not addressed. Erpolat et al. (2004a) used the P–M law and the extended P–M law, in which cycles below the endurance limit also contribute to damage accumulation, to predict failure in an epoxy-CFRP double-lap joint subjected to a variable amplitude (VA) fatigue spectrum. The resulting Miner's sum was significantly less than 1, varying between 0.04 and 0.3, and decreased with increasing load. This indicates that load sequencing is causing damage acceleration, i.e., that the P–M rule is nonconservative in this case.

Some materials exhibit a stress level below which fatigue failure will not occur, known as the fatigue or fatigue limit. In this case, it may be possible to use the data from one sample to predict the fatigue limit for a different geometry or loading condition. A useful method is to experimentally determine the fatigue limit using a calibration sample and to then calculate the value of a suitable failure parameter at the fatigue limit. The fatigue limit can then be predicted for different geometries for failure in the same material by determining the load at which the fatigue limit value of the chosen failure parameter is reached in the new geometry. This is a potentially attractive method as the fatigue threshold value of the chosen failure criterion can be determined from an inexpensive test and then used to predict the fatigue limit for joints that would be expensive to test experimentally. However, in practice, there are the same difficulties as those in the prediction of the quasistatic failure load of adhesive joints, i.e., selection of an appropriate and robust failure criterion, dealing with the theoretical stress singularities, scaling issues and differences in the stress conditions in the simple test and application joints. Abdel Wahab et al. (2001a) predicted the fatigue threshold in CFRP-epoxy lap joints using a variety of stress-and-strain-based failure criteria, taking the value of stress and strain at a distance of

0.04 mm from the singularity to avoid mesh sensitivity. They also used the plastic zone size as a failure criterion.

Under high stress amplitudes, plastic deformation occurs and the fatigue life is considerably shortened. This is known as "low cycle fatigue" (LCF). Coffin (1954) and Manson (1954) proposed that N_f could be related to the plastic strain amplitude, $\Delta\varepsilon_p/2$, in the LCF region.

$$\frac{\Delta\epsilon_p}{2} = B(N_f)^{\beta} \tag{2}$$

where B and β are material constants. The strain–life approach is more difficult to implement than the stress–life method as plastic strain is difficult to measure, particularly for nonhomogenous material systems such as bonded joints. Also, structural joints tend to be used in HCF applications, and hence the strain–life method has seen little application to adhesively bonded joints. Abdel Wahab et al. (2010a, b) proposed a low cycle fatigue damage law based on continuum damage mechanics and applied this to bulk adhesive samples and single-lap joints.

33.4.2 Phenomenological Methods

In the phenomenological approach, fatigue damage is characterized as a function of a measurable parameter, most commonly the residual strength or stiffness after fatigue damage. The reduction in stiffness with fatigue damage, known as stiffness wearout, has the advantage that it can be measured nondestructively; however, it is not directly linked to a failure criterion and may not be very sensitive to the early stages of damage. The strength wearout method provides a useful characterization of the degradation of residual strength, but requires extensive destructive testing. In the strength wearout method, the joint's strength is initially equal to the static strength, S_u, but decreases to $S_R(n)$ as damage accumulates through the application of n fatigue cycles. This degradation can be represented by:
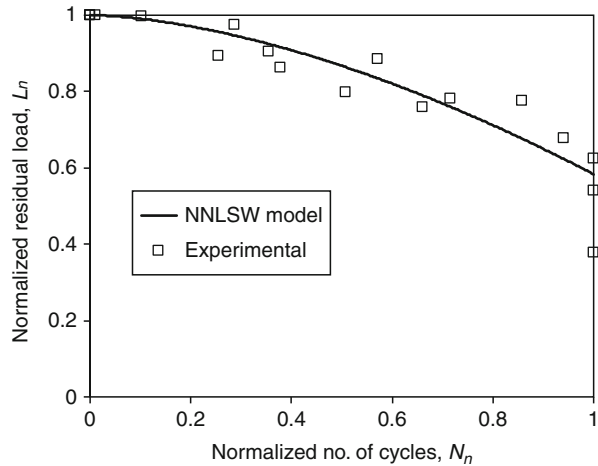
$$S_R(n) = S_u - f(S_u, S_{max}, R)n^{\kappa} \tag{3}$$

where κ is a strength degradation parameter, S_{max} is the maximum stress, and R is the ratio of minimum to maximum stress (i.e., $R = S_{min}/S_{max}$). Failure occurs when the residual strength equals the maximum stress of the spectrum, i.e., when $S_R(N_f) = S_{max}$.

Shenoy et al. (2009b) proposed a modified version of this equation that they termed the normalized nonlinear strength wearout model (NNLSWM), which is given by:

$$L_n = 1 - \frac{(L_u - L_{max})}{L_u}(N_n)^{\eta} \tag{4}$$

where η is a constant and the normalized residual failure load, L_n, is:

$$L_n = \frac{L_R(n)}{L_u}$$

and the normalized cycles to failure, N_n, is:

$$N_n = \frac{n}{N_f}$$

where $L_R(n)$ is the quasistatic failure load after n fatigue cycles and L_u is the quasistatic failure load prior to fatigue loading. Figure 7 shows this model applied to aluminum alloy-epoxy single-lap joints tested at three different fatigue loads. It can be seen that the model fits all the data reasonable well, thus providing a simple method of predicting the residual strength in a joint under any combination of constant fatigue load and number of cycles. However, if the fatigue load varies, modifications to this approach may be required, as discussed in the next section.

Schaff and Davidson (1997a, b) used the strength wearout method to predict the residual strength degradation of a composite material subjected to a variable amplitude loading spectrum. However, they noted a crack acceleration effect in the transition from one constant amplitude (CA) block to another, the cycle mix effect, and proposed a cycle mix factor, CM, to account for this. Erpolat et al. (2004a) proposed a modified form of Shaff and Davidson's cycle mix equation to model the degradation of CFRP-epoxy double-lap joints subjected to a variable amplitude fatigue spectrum. They showed that this model represented the fatigue life of bonded joints under variable amplitude fatigue more accurately than Palmgren–Miner's law. Shenoy et al. (2009c) proposed various further modifications to this approach, which they applied to aluminum alloy-epoxy single-lap joints subjected to various forms of VAF. The application of the cycle mix factor to predict strength wearout and cycles
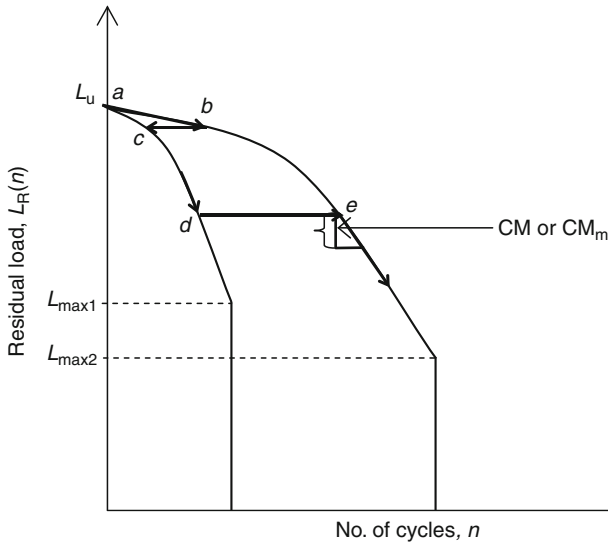
Fig. 8 Illustration of the nonlinear strength wearout with cycle mix factor approach to predict variable amplitude fatigue

to failure for VAF is illustrated in Fig. 8. The figure shows two strength wearout curves, showing the reduction in the residual load for constant amplitude fatigue with maximum fatigue loads of L_{max1} and L_{max2}. Both of these curves can be represented by a nonlinear strength wearout equation, such as Eq. (4). If a variable amplitude fatigue spectrum commences with a maximum fatigue load of L_{max2}, then the decrease in the residual load with fatigue cycles initially follows path a–b. If at point b the maximum fatigue load increases to L_{max1}, there is a horizontal jump to the strength wearout curve for the higher load and the residual load starts to decrease more quickly, following curve c–d. At point d, the maximum load is decreased to L_{max2}, and we have another horizontal jump to the relevant strength wearout curve. However, at point e, the cycle mix factor is also applied, which has the effect of an immediate reduction in the residual load by an amount CM (or CM_m). Shenoy et al. (2009c) proposed two cycle mix factors. The first was the cycle-independent cycle mix factor used by Erpolat et al. (2004a) given in Eq. (5).

$$\mathrm{CM} = \alpha\left[(\Delta L_{mn})^{\beta L_{max}\left(\Delta L_{max,1}/\Delta L_{mn,1}\right)^{\gamma}}\right] \tag{5}$$

ΔL_{mn} and ΔL_{max} are the mean and maximum load changes during the transition from one mean load to the other, α and β are experimentally determined parameters, and γ was assumed to be unity in this case. The second was termed the modified cycle mix factor (MCM) approach. This was developed after observing that a better fit to the experimental data could be made if the cycle mix factor was greater in the

low cycle regime than in the high cycle regime. As it had already been noted that with these joints the fatigue life was propagation dominated in the low cycle regime and initiation dominated in the high cycle regime, the desired effect was achieved by making the cycle mix factor dependent on the extent of damage in the sample, as shown in Eq. (6).

$$\text{CM}_\text{m} = \left(\frac{\zeta}{\text{OL}} + \alpha\right)\left[(\Delta L_\text{mn})^{\beta L_\text{max}(\Delta L_\text{max}/\Delta L_\text{mn})^y}\right] \tag{6}$$

where OL is the overlap length and ζ is a damage parameter. In Shenoy et al. (2009c), ζ was determined by fitting a power law curve to experimental plots of damage/crack growth against number of cycles. Hence, ζ was defined as:

$$\zeta = m_1(n)^{m_2} \tag{7}$$

where m_1 and m_2 are experimentally determined constants.

It can be seen in Fig. 9 that the cycle mix parameter was applied when the fatigue loading became less severe, i.e., after the jump from d to e, but not when the fatigue loading became more severe, i.e., following the jump from b to c. This is consistent with Gomatam and Sancaktar (2006) who observed damage acceleration when "moderate" loading conditions followed "severe" loading conditions, but not when the order was reversed. It is also consistent with the mechanistic argument put forward by Ashcroft (2004) who attributed crack growth accelerations seen in adhesives subjected to intermittent overloads to the damage caused by the overloads to the adhesive ahead of the crack tip. It was proposed that this damage reduced the fatigue resistance of the adhesive and resulted in accelerated crack growth for the cycles of lower amplitude following an overload.

Fig. 9 Experimental fatigue crack growth curve for a CFRP-epoxy double cantilever beam (Data from Ashcroft and Shaw 2002)
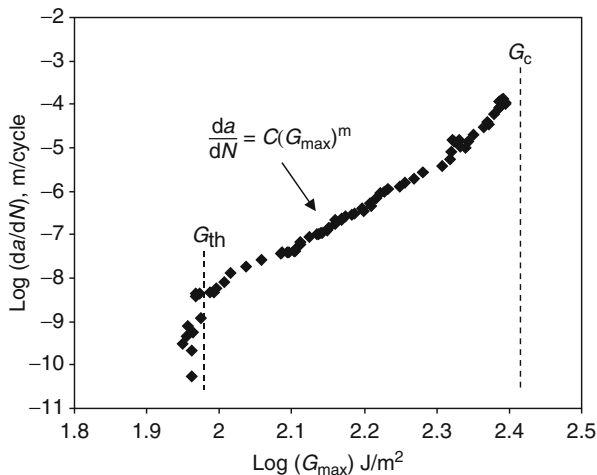
As with strength degradation, stiffness degradation rate can be considered as a power function of the number of load cycles. Although stiffness degradation has the advantage that it can be measured nondestructively, it does not give a direct indication of the residual strength of a fatigued structure. However, if this link can be made, then stiffness degradation can be a useful method of in-service structural integrity monitoring.

33.4.3 Fracture Mechanics Methods

The fracture mechanics approach deals predominantly with the crack propagation phase; hence, it is assumed that crack initiation occurs during the early stages of the fatigue cycling or that there is a preexisting crack. The rate of fatigue crack growth, da/dN, is then correlated with an appropriate fracture mechanics parameter, such as Griffith's (1921) strain energy release rate, G, or Irwin's (1958) stress intensity factor, K. Paris et al. (1961) proposed that da/dN was a power function of the stress intensity factor range, $\Delta K (= K_{max} - K_{min})$, i.e.:

$$\frac{\mathrm{d}a}{\mathrm{d}N} = C\Delta K^m \tag{8}$$

where C and m are empirical constants, dependent on factors such as the material, the fatigue frequency, the R-ratio, and environment. Although K is the most widely used fracture mechanics parameter in the fracture analysis of metals, it is more difficult to apply to bonded joints, where the constraint effects of the substrates on the adhesive layer complicates characterization of the stress field around the crack tip. Therefore, G is often used as the governing fracture parameter for adhesives if linear elastic fracture mechanics (LEFM) is applicable (i.e., localized plasticity). If an elastoplastic fracture mechanics (EPFM) parameter is required, owing to more widespread plasticity, then the J-integral (J) is generally used (Rice 1968). If creep is significant, then a time-dependent fracture mechanics parameter, such as C^* or C_t, should be considered, as discussed in Sect. 5.

A plot of the experimentally measured crack growth rate against the calculated G_{max} or ΔG often exhibits three regions, as illustrated in Fig. 9, which shows the fatigue crack growth curve for a CFRP-epoxy double cantilever beam (DCB). Region I is defined by the threshold strain energy release rate, G_{th}, in which crack growth is slow enough to be deemed negligible. Region II is described by a power law equation similar to Eq. (6) and is, hence, sometimes referred to as the Paris Region. In Region III, there is unstable fast crack growth as G_{max} approaches the critical strain energy release rate, G_c.

In a general form, the relationship between the fatigue crack propagation rate and a relevant fracture parameter, Γ, can be represented by:

$$\frac{\mathrm{d}a}{\mathrm{d}N} = f(\Gamma) \tag{9}$$

The number of cycles to failure can be determined from:

$$N_f = \left(\int_{a_0}^{a_f} \frac{da}{f(\Gamma)} \right) \tag{10}$$

where a_0 is the initial crack length and a_f is the final crack length. Equation (10) can be solved using numerical crack growth integration (NCGI). A simple method of predicting VA fatigue from a CA FCG curve is to perform numerical crack growth integration. In this method, the crack size, a, and corresponding fracture parameter, such as strain energy release rate range, ΔG, is assumed to be constant throughout a CA stage. The crack growth rate per cycle, da/dN, for this stage can be obtained using an appropriate correlation, such as the Paris law. Multiplication of this rate by the number of cycles in the stage, n, gives the overall crack growth during the stage, Δa. This is used to find the crack size for the subsequent stage ($a_{i+1} = a_i + \Delta a_i$) and the procedure is repeated until G_{max} exceeds the fracture energy, G_c, or until ΔG becomes equal to ΔG_{th}. This algorithm is summarized below.

Repeat

$$a_{i+1} = a_i + n_i \cdot \frac{da}{dN}\left(\Delta G_i(R_i, a_i, \ldots) \right) \tag{11}$$

Until $G_{max,\, i+1} \geq G_c$ {G increasing with a} or
Until $\Delta G_{max,\, i+1} \leq \Delta G_{th}$ {G decreasing with a}

Abdel Wahab et al. (2004) proposed a general method of predicting fatigue crack growth and failure in bonded lap joints incorporating NCGI and finite element analysis (FEA). The crack growth law was determined from tests using a DCB sample and this was used to predict the fatigue crack growth, and hence the fatigue life, of single- and double-lap joints manufactured from the same materials.

The numerical integration technique can easily be adapted to the prediction of fatigue crack growth in variable amplitude (VA) fatigue. Erpolat et al. (2004b) applied the NCGI technique for the prediction of crack growth in CFRP/epoxy DCB joints subjected to periodic overloads. This tended to underestimate the experimentally measured crack growth, indicating a crack growth acceleration mechanism, and an unstable, rapid crack growth period was also seen when high initial values of G_{max} were applied. This behavior was attributed to the generation of increased damage in the process zone ahead of the crack tip when the overloads were applied, and Ashcroft (2004) proposed a fracture mechanics-based model that could predict this behavior. It was assumed that under constant amplitude conditions, FCG can be represented by ΔG_{th}, G_C, and the two Paris constants, C and m, as represented by CA in Fig. 10. It can be seen that if a CA fatigue load with a strain energy release rate range of ΔG_A is applied, then the resulting crack growth rate will be $(da/dN)_{CA}$. In most cases, ΔG_A will be calculated assuming undamaged material ahead of the crack tip, and this is likely to be adequate for predictive purposes. However, the crack resistance and hence $(da/dN)_{CA}$ will be associated with the damage zone

Fig. 10 The damage shift method of predicting fatigue crack growth under variable amplitude (Ashcroft 2004)
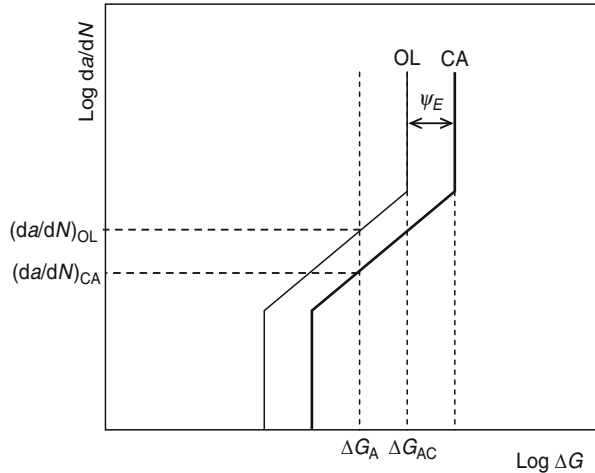
created by the CA fatigue loading. If an overload is superimposed onto the CA spectrum, then the damage ahead of the crack zone will increase and the resistance to crack propagation will decrease. It is proposed that this increased damage can be represented by a lateral shift in the FCG curve. The FCG curve associated with this increased damage is represented by curve OL in Fig. 10. It can be seen that the value of da/dN at ΔG_A has increased to $(da/dN)_{OL}$, i.e., that there is a crack acceleration effect, which is represented by a "damage shift" parameter, ψ_E, which can be easily determined for a given spectrum through a simple experimental test program. Theoretically, all that is needed to determine ψ_E is the crack growth rates under CA and VA fatigue for a single value of ΔG_A.

If ΔG_A is increased, a critical point will eventually be reached at which G_{max} of the overloads is equal to the value of G_c for the shifted FCG curve, OL. This point is shown as ΔG_{AC} in Fig. 10. Unstable or quasistatic fracture then occurs. If G increases with crack length, then this will lead to catastrophic failure of the joint. However, if G decreases with a, as when testing DCB samples in displacement control, then the crack will eventually stop if the G arrest (G_{arr}) value is reached before the joint has completely fractured. The value of ΔG_A associated with the crack arrest point (ΔG_{arr}) will now be much smaller, and hence crack growth will be greatly reduced. This is consistent with the experimental crack growth behavior shown in Fig. 11, where there is a rapid increase in crack length after approximately 5000 fatigue cycles, after which there is a period of lower crack growth rate than that predicted by NCGI. It can be seen in Fig. 11 that the damage shift model is capable of predicting both the initial crack jump and the subsequent reduction in the crack growth rate.

The fatigue crack growth approach will only predict the correct fatigue life if it is dominated by the fatigue propagation phase. However, if the initiation phase is significant, then this approach will underestimate the fatigue life and a method of predicting the number of cycles before the macrocrack forms is required. This can be done empirically in a similar fashion to the stress–life approach, with the number of

Fig. 11 Fatigue crack growth for CFRP-epoxy DCB subjected to overloads
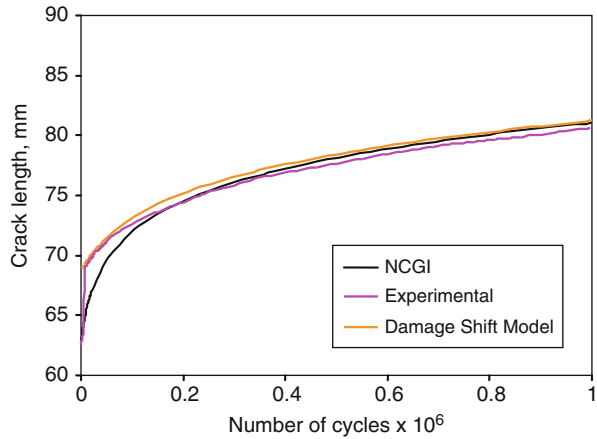
cycles to fatigue initiation, N_i, being plotted as a function of a suitable stress (or other) parameter rather than cycles to total failure, N_f (Shenoy et al. 2009a). An alternative approach, suggested by Levebvre and Dillard (1999), is to use a stress singularity parameter as the fatigue initiation criterion. They showed that under certain conditions, the singular stress, σ_{kl}, in an adhesive lap joint could be represented by:

$$\sigma_{kl} = \frac{Q_{kl}}{x^\lambda} \qquad (12)$$

where Q_{kl} is a generalized stress intensity factor, dependent on load, and λ is an eigenvalue that can be related to the order of the singularity. It was proposed that N_i could be defined in terms of ΔQ (or Q_{max}) and λ in a 3D failure map. This approach has been combined with a fracture mechanics approach by Quaresimin and Ricotta (2006) to obtain a predictive method explicitly modeling both the initiation and propagation phases. An alternative to this is to use one of the damage mechanics methods described in Sect. 4.4.

Adhesives and polymer composites tend to exhibit fast fracture, and hence it may be preferable to design for a service life with no crack growth, using G_{th} as the design criteria. Abdel Wahab et al. (2001a) investigated this approach for bonded lap-strap joints. Elastic (G) and elastoplastic (J) fracture parameters, crack placement, and initial crack size were investigated. This approach has also been extended to samples subjected to environmental ageing by incorporating the method with a semicoupled transient hygromechanical finite element analysis (Ashcroft et al. 2003). Ashcroft and Shaw (2002) used G_{th} from testing DCB joints to predict the 10^6 cycle endurance limit in lap-strap and double-lap joints at different temperatures. The predictions were reasonable, apart from the double-lap joint tested at 90 °C, which failed at a far lower load than predicted. This was attributed to accumulative creep in the double-lap joint, which could be seen in plots of displacement against cycles at constant load amplitude.
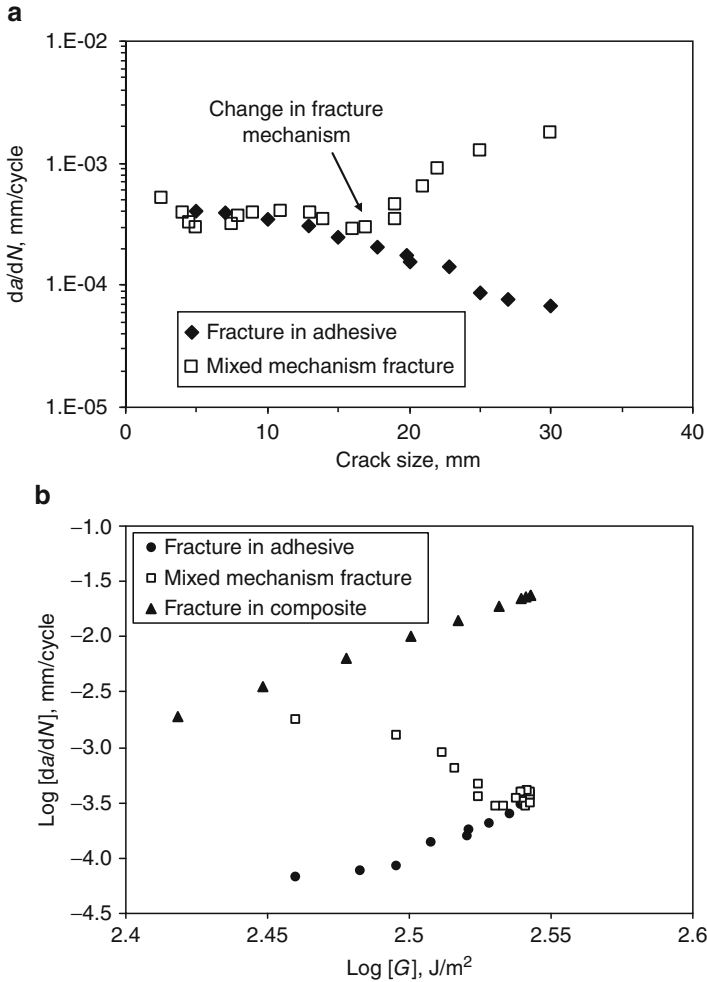
Fig. 12 (**a**) Fatigue crack growth rate as a function of crack length for fracture in the adhesive and a mixed mechanism fracture. (**b**) Fatigue crack growth plots for fracture in the adhesive layer in the composite and a mixed mechanism fracture

It is quite common in adhesively bonded joints to have more than one failure mechanism, for example, cohesive failure in the adhesive, failure at the interface, interlaminar failure, or matrix failure in composite substrates, occurring in the fatigue life of a joint. This will affect the fatigue crack growth, as illustrated in Fig. 12a. If the various mechanisms occur sequentially, then failure criteria for the joint can also be applied sequentially in a fatigue lifetime predictive methodology. However, if more than one mechanism is occurring at one time, anomalous fatigue crack growth can occur. This is illustrated in Fig. 12b for the case of a CFRP-epoxy lap-strap joint in which fracture is initially in the adhesive before developing into a

mixed mechanism failure with an increasing proportion of failure in the composite adherend. It can be seen that in the mechanism fracture, the fatigue crack growth exhibits anomalous behavior as the crack growth rate decreases as strain energy release rate increases, which is not represented by a Paris-type crack growth law. Ashcroft et al. (2010) proposed a mixed mechanism fracture model of the following form:

$$\left(\frac{\mathrm{d}a}{\mathrm{d}n}\right)_\mathrm{m} = f\left[A_\mathrm{a}, \left(\frac{\mathrm{d}a}{\mathrm{d}n}\right)_\mathrm{a}, A_\mathrm{c}\left(\frac{\mathrm{d}a}{\mathrm{d}n}\right)_\mathrm{c}\right] \tag{13}$$

where A indicates area fraction of failure mode, as seen in the fracture surface, and the subscripts m, a, and c represent mixed, adhesive, and composite, respectively. The simplest form of this law is a simple additive one, i.e.:

$$\left(\frac{\mathrm{d}a}{\mathrm{d}n}\right)_\mathrm{m} = A_\mathrm{a}\left(\frac{\mathrm{d}a}{\mathrm{d}n}\right)_\mathrm{a} + A_\mathrm{c}\left(\frac{\mathrm{d}a}{\mathrm{d}n}\right)_\mathrm{c} \tag{14}$$

Equation (14) assumes there is a proportional relationship between the area fraction of a particular failure mode and its effect on the mixed FCG rate; however, this is not necessarily the case. It may be the case that one of the fracture mechanisms has a disproportionate effect on the mixed FCG rate. A simple way to accommodate this is to substitute the actual area fraction, A_i, in Eq. (14) with an effective area fraction, A_i', as illustrated in Eq. (15)

$$\left(\frac{\mathrm{d}a}{\mathrm{d}n}\right)_\mathrm{m} = A_\mathrm{a}'\left(\frac{\mathrm{d}a}{\mathrm{d}n}\right)_\mathrm{a} + A_\mathrm{c}'\left(\frac{\mathrm{d}a}{\mathrm{d}n}\right)_\mathrm{c} \tag{15}$$

A method of mapping the actual area fraction to the effective area fraction is required, and Ashcroft et al. (2010) illustrated how power laws and polynomial relationships could be used for this purpose. It was shown that the proposed model was capable of predicting the anomalous fatigue crack growth behavior shown in Fig. 12.

33.4.4 Damage Mechanics Methods

The fracture mechanics methods have the limitation that the initiation phase is not accounted for and that damage is through a single planar crack propagating through undamaged material, which may not physically represent the real behavior very well. The damage mechanics approach addresses some of these problems by allowing progressive degradation and failure to be modeled, thus representing both initiation and propagation phases. Continuum damage mechanics (CDM) requires a damage variable, D, to be defined as a measure of the severity of the material damage, where D is equal to 0 for undamaged material and 1 for fully damaged material. Abdel Wahab et al. (2001b) developed the following fatigue damage equation:

$$D = 1 - \left[1 - A(\beta + m + 1)\Delta\sigma_{\mathrm{eq}}{}^{\beta+m}R_{\mathrm{v}}{}^{\beta/2}N \right]^{\frac{1}{\beta+m+1}} \tag{16}$$

where $\Delta\sigma_{\mathrm{eq}}$ is the von Mises stress range, R_{v} is the triaxiality function (which is the square of the ratio of the damage equivalent stress to the von Mises equivalent stress), m is the power constant in the Ramberg–Osgood equation, and A and β are experimentally determined damage parameters. The number of cycles to failure (N_{f}) can be determined from Eq. (16) using the condition at the fully damaged state, $D = 1$ at $N = N_{\mathrm{f}}$, giving:

$$N_{\mathrm{f}} = \frac{\Delta\sigma_{\mathrm{eq}}{}^{-\beta-m}R_{\mathrm{v}}{}^{-\frac{\beta}{2}}}{A(\beta + m + 1)} \tag{17}$$

Abdel Wahab et al. (2001b) found that the approach described above compared favorably with the fracture mechanics approach when applied to the constant amplitude fatigue of CFRP-epoxy double-lap joints. Abdel Wahab et al. (2010a) later extended this approach to the low cycle fatigue of bulk adhesive where damage evolution curves were derived assuming isotropic damage and a stress triaxiality function equal to one that agreed well with experimental measurements. In further work, Abdel Wahab et al. (2010b) applied the approach to single-lap joints which required determination of the triaxiality function to account for the multiaxial stress state in the joint, and it was seen that this value varied along the adhesive layer. The dependency of the triaxiality function on the joint type was further investigated by Abdel Wahab et al. (2011a, b).

Although the CDM approach described above enabled the progressive degradation of the adhesive layer to be characterized, it did not allow the initiation and propagation phases of fatigue to be explicitly modeled. Shenoy et al. (2010a) used a damage mechanics-based approach to progressively model the initiation and evolution of damage in an adhesive joint, leading to crack formation and growth. In this approach, the damage rate dD/dN was assumed to be a power law function of the localized equivalent plastic strain range, $\Delta\varepsilon_{\mathrm{p}}$, i.e.:

$$\frac{dD}{dN} = C_{\mathrm{D}}\left(\Delta\epsilon_{\mathrm{p}}\right)^{m}\mathrm{D} \tag{18}$$

where C_{D} and m_{D} are experimentally derived constants. The fatigue damage law was implemented in a finite element model. In each element, the rate of damage was determined from the finite element analysis using Eq. (18), and the element properties degraded as:

$$E = E_0(1 - D)$$

$$\sigma_{\mathrm{yp}} = \sigma_{\mathrm{yp0}}(1 - D) \tag{19}$$

$$\beta = \beta_0(1 - D)$$

where E_0, σ_{yp0}, and β_0 are Young's modulus, yield stress, and plastic surface modifier constant for the Parabolic Mohr–Coulomb model, respectively, and $D = 1$ represents a fully damaged element, which was used to define the macrocrack length. The fatigue life was broken into a number of steps with a specified number of cycles, ΔN, and at each step, the increased damage determined using Shenoy et al. (2010a):

$$D_{i+1} = D_i + \frac{dD}{dN} dN \tag{20}$$

showed that this method could be used to predict total-life plots, the fatigue initiation life, fatigue crack growth curves, and strength and stiffness wearout plots and could also be extended to variable amplitude fatigue (Shenoy et al. 2010b). Walander et al. (2014) experimentally studied Mode-I fatigue crack growth in rubber and polyurethane-based adhesives using a double-cantilever beam specimen. A damage growth law of a similar form to Eq. (20) related damage evolution with three material parameters: α, β, and σ_{th}, which were determined from the experimental data. Good correlation between the experimental data and the proposed damage law for fatigue was reported.

A similar approach was proposed by Khoramishad et al. (2010a) in which the rate of damage was related to the maximum principal strain, ϵ_{max}, rather than the equivalent strain and a threshold strain, ϵ_{th}, was used rather than a plastic strain in order to define a strain below which fatigue damage does not occur.

$$\frac{\Delta D}{\Delta N} = \begin{cases} C \times (\epsilon_{max} - \epsilon_{th})^b, & \epsilon_{max} > \epsilon_{th} \\ 0, & \epsilon_{max} \leq \epsilon_{th} \end{cases} \tag{21}$$

where C and b are experimentally determined material damage constants. In this case, the damage initiation and fracture was modeled using a bilinear cohesive zone model (as described in ▶ Chap. 25, "Numerical Approach: Finite Element Analysis") and the damage variable was used to degrade the parameters of the cohesive model as illustrated in Fig. 13. This method was later extended to incorporate the effect of varying load ratio (Khoramishad et al. 2010b), variable amplitude fatigue (Khoramishad et al. 2011), and the effect of moisture degradation (Katnam et al. 2011).

Pirondi and Moroni (2010) also proposed a method of predicting fatigue crack growth using cohesive zone elements within a finite element analysis. In this case, the damage rate was related to the strain energy release rate. Oinen and Marquis (2011) presented a damage model for the shear decohesion of combined clamped and adhesively bonded (i.e., hybrid) joints that incorporated a linear-exponential cohesive zone model and a frictional contact model to account for a combined slip and decohesion response to loading.

33.5 Creep-Fatigue

Evidence of creep in the fatigue testing of bonded lap joints has been observed by a number of authors. It was seen in Sect. 4.3 that application of a standard fracture mechanics method can significantly overpredict the fatigue life if there is
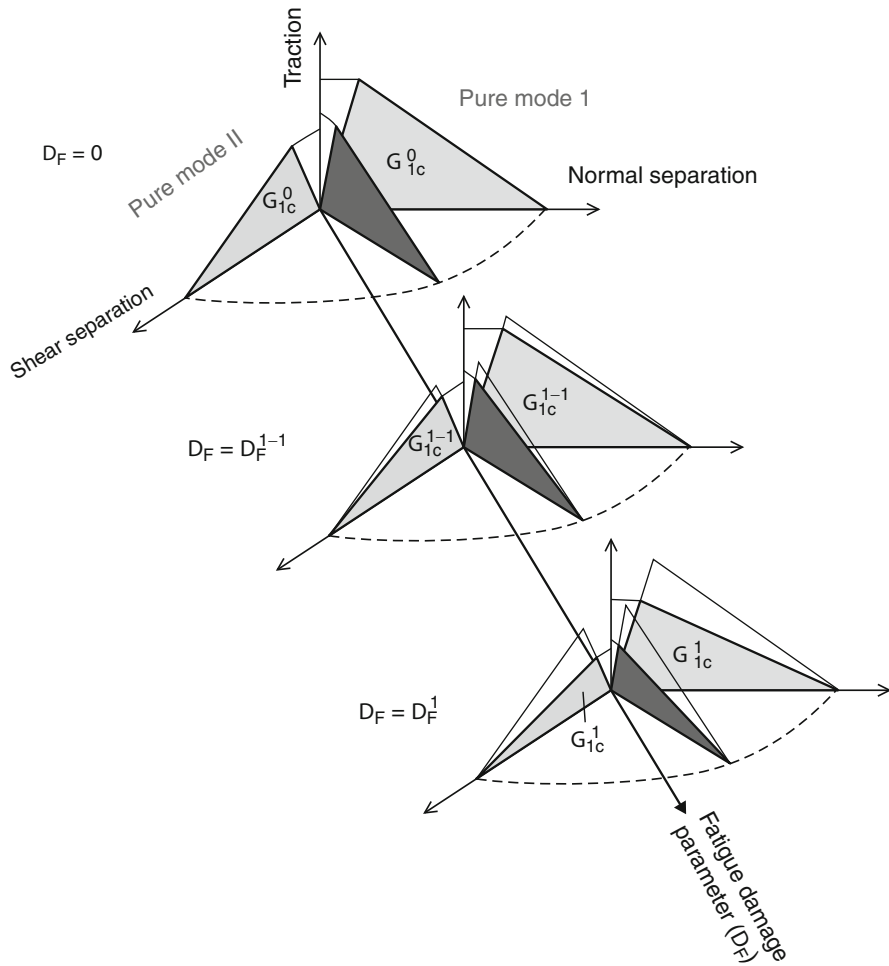
Fig. 13 Degradation of cohesive zone model parameters with increasing fatigue damage (Khoramishad et al. 2010a)

significant accumulated creep. This is not surprising as polymeric adhesives will exhibit some degree of viscoelastic or viscoplastic behavior over a part of their operating range. The importance of the creep contribution to fatigue failure will depend on a number of factors such as the nature of the adhesive, the ambient temperature and humidity, the joint geometry, the mean fatigue load, and the frequency. Fatigue crack growth in such circumstances may still be adequately represented by LEFM or EPFM parameters; however, different fatigue crack growth curves will be required for different frequencies and temperatures, as shown in Fig. 14. However, if creep is significant, then fatigue crack growth may be better represented by a time-dependent fracture mechanics (TDFM)

Fig. 14 The effect of test frequency on fatigue crack growth plots for steel-epoxy DCB samples (Al-Ghamdi et al. 2003)
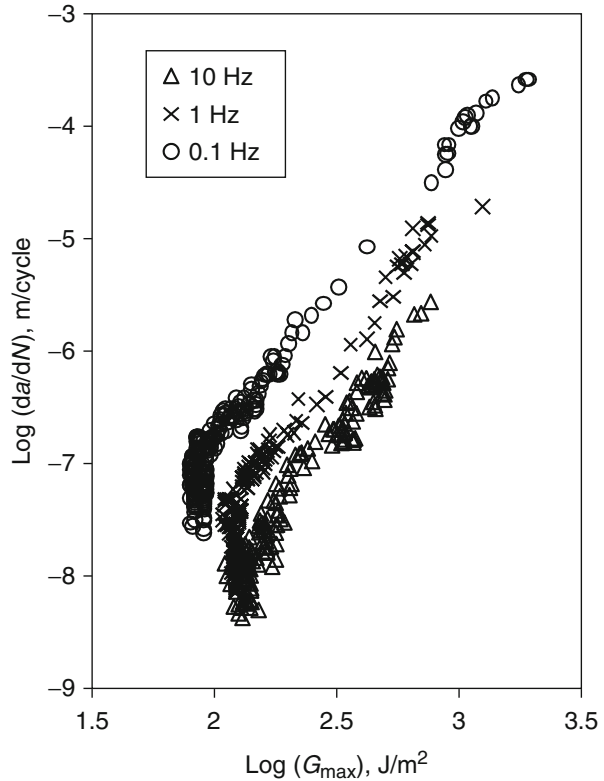
parameter. Landes and Begley (1976) proposed a TDFM parameter analogous to
Rice's J-integral that they called C^* and defined it as follows:

$$C^* = \int_{\Gamma} W^* dy - T_i \left\{ \partial \frac{\dot{u}}{\partial x} \right\} ds \tag{22}$$

where

$$W^* = \int_0^{\dot{\epsilon}_{ij}} \sigma_{ij} d\dot{\epsilon}_{ij} \tag{23}$$

Γ is a line contour taken counter clockwise from the lower crack surface to the
upper crack surface, W^* is the strain energy rate density associated with the stress σ_{ij}
and strain rate $\dot{\epsilon}_{ij}$, T_i is the traction vector defined by the outward normal n along Γ, $\dot{u}_i$
is the displacement rate vector, and s is the arc length along the contour. C^* is valid

only for extensive steady-state creep condition, and Saxena (1986) proposed an alternative parameter, C_t, that was suitable for characterizing creep crack growth from small scale to extensive creep conditions. This was defined as:

$$C_t = -\frac{1}{B} \partial U_t^* \left(\frac{a, t, \dot{V}_c}{\partial a} \right) \tag{24}$$

where B is sample width, a is crack length, t is time, U_t^* is an instantaneous stress–power parameter, and $\dot{V}_c$ is the load line deflection rate.

In cyclic loading, C_t will vary with the applied load, and an average value of C_t, $C_{t\ (ave)}$, may be used to characterize the fatigue-creep crack growth. Al-Ghamdi et al. (2004) proposed three methods of predicting creep-fatigue crack growth in bonded joints. In the first method, an appropriate fracture mechanics parameter is selected and plotted against the fatigue crack growth rate (FCGR = da/dN) or the creep crack growth rate (CCGR = da/dt). A suitable crack growth law is fitted to the experimental data and crack growth law constants are determined at different temperatures and frequencies. Empirical interpolation can then be used to determine crack growth law constants at unknown temperatures and frequencies. This method can also be used to predict crack growth under conditions of varying frequency, load, and temperature.

The second method was called the *dominant damage approach* and assumes that fatigue and creep are independent mechanisms and that crack growth is determined by whichever is dominant. In this case, crack growth should be predominantly either cycle or time dependent. For example, if creep is the dominant damage mechanism, then plots of da/dt against a suitable TDFM should be independent of frequency and can be used to predict the fatigue life in terms of time under load rather than number of cycles.

The third method was termed the *crack growth partitioning approach* in which it is assumed that crack growth can be partitioned into separate cycle-dependent (fatigue) and time-dependent (creep) components, both of which contribute the total crack, as represented by the following equation:

$$\frac{da}{dN} = \left(\frac{da}{dN} \right)_{fatigue} + \frac{1}{f} \left(\frac{da}{dt} \right)_{creep} \tag{26}$$

Al-Ghamdi et al. (2004) proposed the following form of Eq. (26):

$$\frac{da}{dN} = D(G_{max})^n + \frac{mC_{t(ave)}^q}{f} \tag{27}$$

where the fatigue crack growth constants D and n are determined from high-frequency tests, and the creep crack growth constants m and q are determined from constant load crack growth tests. Under some conditions, this method still underpredicts the crack growth, in which case a creep-fatigue interaction term may be added:

$$\frac{\mathrm{d}a}{\mathrm{d}N} = D(G_{\max})^n + \frac{mC_{t(\mathrm{ave})}^q}{f} + \mathrm{CF}_{\mathrm{int.}} \tag{28}$$

where $\mathrm{CF}_{\mathrm{int.}} = R_{\mathrm{f}}^p R_{\mathrm{c}}^y C_{\mathrm{fc}}$ and R_{f} and R_{c} are scaling factors for the cyclic and time-dependent components, respectively.

$$R_{\mathrm{f}} = \frac{(\mathrm{d}a/\mathrm{d}N)}{(\mathrm{d}a/\mathrm{d}N) + (\mathrm{d}a/\mathrm{d}t)/f}$$

$$R_{\mathrm{c}} = \frac{(\mathrm{d}a/\mathrm{d}t)/f}{(\mathrm{d}a/\mathrm{d}N) + (\mathrm{d}a/\mathrm{d}t)/f}$$

and p, y, and C_{fc} are empirical constants.

33.6   Impact Fatigue

There is increasing interest in the effects of repetitive low-velocity impacts produced in components and structures by vibrating loads. This type of loading is known as impact fatigue. Typical plots of normalized force as a function of time from the impact fatigue testing of a bonded single-lap joint are shown in Fig. 15. It can be seen that the duration of the main peak is approximately 2 ms and that subsequent peaks are of significantly smaller magnitude. It can also be seen that the maximum force, $F_{\max}$, and the load time for the first peak, T_{F}, decrease with the number of cycles, which is indicative of progressive fatigue damage in the adhesive. As the force is not constant in an impact fatigue test, it is useful to define a mean maximum force $\overline{F}_{\max}$ as:
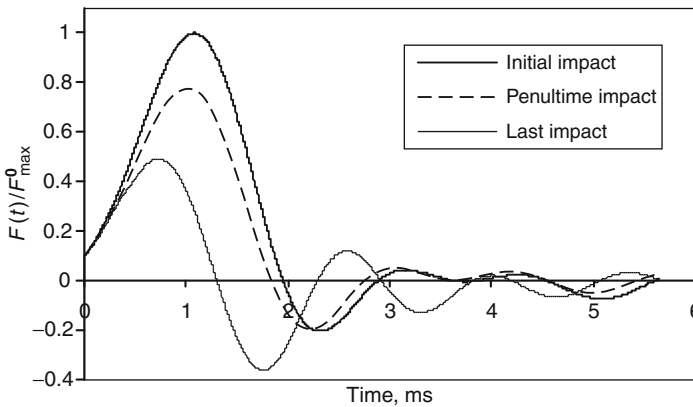

Fig. 15 Variation in force and strain with time in a typical impact in the impact fatigue testing of a bonded lap joint (Casas-Rodriguez et al. 2007)
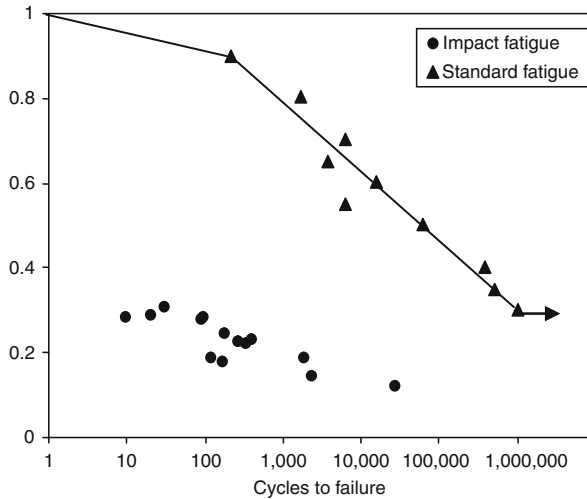
Fig. 16 *F–N* diagrams for aluminum-epoxy single-lap joints in impact and standard fatigue (Casas-Rodriguez et al. 2007)

$$\overline{F}_{\max} = \frac{1}{N_{\mathrm{f}}} \sum_{i=1}^{N_{\mathrm{f}}} F_i^{\max} \qquad (29)$$

In Fig. 16, the normalized mean maximum force is plotted against the logarithm of cycle to failure and it can be seen that an approximately linear relationship is observed, with cycles to failure increasing as the force decreases, as expected. A plot for similar single-lap joints, manufactured with the same materials and processes, tested in standard fatigue with a constant force amplitude, sinusoidal waveform can also be seen in Fig. 16. It can be seen from this that the impact fatigue appears to be significantly more damaging than the standard fatigue. Casas-Rodriguez et al. (2008) also compared damage and crack growth in CFRP-epoxy lap-strap joints in standard and impact fatigue and found that the accumulated energy associated with damage in impact fatigue was significantly lower than that associated with similar damage in standard fatigue. It was also seen that the fracture surfaces, and hence, the fracture mechanisms, were quite different for the two types of loading. Ashcroft et al. (2011) also investigated the impact fatigue of notched bulk adhesive samples, developing an impact fatigue growth law based on the dynamic strain energy release rate.

33.7 Conclusion

It can be seen that a number of techniques have been used to model fatigue in bonded joints. Although most methods have limitations, all are useful in understanding and/or characterizing the fatigue response of bonded joints, and it is expected that further

developments will continue in all the methods described. For instance, the traditional load–life approach is useful in characterizing global fatigue behavior, but is of little use in fatigue life prediction and provides no useful information on damage progression in the joint. However, combined with monitoring techniques, such as back-face strain or embedded sensors, and FEA, the method could potentially form the basis of an extremely powerful in-service damage monitoring technique for industry.

The fracture mechanics approach is potentially a more flexible tool than the stress–life approach as it allows the progression of cracking to failure to be modeled and can be transferred to different sample geometries. Problems with the traditional fracture mechanics approach include: selection of initial crack size and crack path, selection of appropriate failure criteria, load history, and creep effects. Also the fracture mechanics approach does not accurately represent the accumulation and progression of damage observed experimentally in many cases. However, recent modifications to the standard fracture mechanics method have seen many of these limitations tackled.

In future developments, it is expected that fatigue studies of bonded joints will continue to increase our knowledge of how fatigue damage forms and progresses in bonded joints and this will feed into the models being developed. In addition to further developments and extension to the approaches described above, it is expected that an area for huge potential advances is in the incorporation of increasingly sophisticated damage growth laws into finite element analysis models to develop a more mechanistically accurate representation of fatigue in bonded joint than is currently available. It is also hoped that many of the techniques described above will reach sufficient maturity to form the basis of useful tools for industry, both in the initial design and in-service monitoring of bonded joints in structural applications subjected to cyclic loading.

References

Abdel Wahab MM, Ashcroft IA, Crocombe AD, Hughes DJ, Shaw SJ (2001a) Compos Part A 32:59

Abdel Wahab MM, Ashcroft IA, Crocombe AD, Hughes DJ, Shaw SJ (2001b) J Adhes Sci Technol 15:763

Abdel Wahab MM, Ashcroft IA, Crocombe AD, Smith PA (2004) Compos Part A 35:213

Abdel Wahab MM, Hilmy I, Ashcroft IA, Crocombe AD (2010a) J Adhes Sci Technol 24:305

Abdel Wahab MM, Hilmy I, Ashcroft IA, Crocombe AD (2010b) J Adhes Sci Technol 24:325

Abdel Wahab MM, Hilmy I, Ashcroft IA, Crocombe AD (2011a) J Adhes Sci Technol 25:903

Abdel Wahab MM, Hilmy I, Ashcroft IA, Crocombe AD (2011b) J Adhes Sci Technol 25:925

Al-Ghamdi AH, Ashcroft IA, Crocombe AD, Abdel Wahab MM (2003) J Adhes 79:1161

Al-Ghamdi AH, Ashcroft IA, Crocombe AD, Abdel-Wahab MM (2004) Proceedings of the 7th international conference on structural adhesives in engineering. IOM Communications, London, pp 22–25

Ashcroft IA (2004) J Strain Anal 39:707

Ashcroft IA, Shaw SJ (2002) Int J Adhes Adhes 22:151

Ashcroft IA, Abdel Wahab MM, Crocombe AD, Hughes DJ, Shaw SJ (2001a) Compos Part A 32:45

Ashcroft IA, Abdel-Wahab MM, Crocombe AD, Hughes DJ, Shaw SJ (2001b) J Adhes 75:61

Ashcroft IA, Abdel-Wahab MM, Crocombe AD (2003) Mech Adv Mater Struct 10:227

Ashcroft IA, Casas-Rodriguez JP, Silberschmidt VV (2010) J Adhes 86:522

Ashcroft IA, Silberschmidt VV, Echard B, Casas-Rodrguez JP (2011) Shock Vib 18:157

Casas-Rodriguez JP, Ashcroft IA, Silberschmidt VV (2007) J Sound Vib 308:467

Casas-Rodriguez JP, Ashcroft IA, Silberschmidt VV (2008) Comp Sci Technol 68:2663

Coffin LF (1954) Trans Am Soc Mech Eng 76:931

Costa M, Viana G, da Silva LFM, Campilho RDSG (2017) J Adhes 93:127

Crocombe AD, Richardson G (1999) Int J Adhes Adhes 19:19

Datla NV, Ulicny J, Carlson B, Papini M, Spelt JK (2011a) Eng Fract Mech 78:1125

Datla NV, Ulicny J, Carlson B, Papini M, Spelt JK (2011b) Int J Adhes Adhes 31:88

Dowling NE (1999) Mechanical behaviour of materials. Prentice Hall, New Jersey, pp 390–392

Erpolat S, Ashcroft IA, Crocombe AD, Abdel Wahab MM (2004a) Int J Fatigue 26:1189

Erpolat S, Ashcroft IA, Crocombe AD, Abdel Wahab MM (2004b) Comp A 35:1175

Farrow IR (1989) Damage accumulation and degradation of composite laminates under aircraft service loading: Assessment and prediction, Vol. I & II. PhD thesis, Cranfield Institute of Technology

Gomatam R, Sancaktar E (2006) J Adhes Sci Technol 20:69

Griffith AA (1921) Phil Trans R Soc A221:163

Irwin GR (1958) Fracture. In: Flugge S (ed) Handbuch der physic VI. Springer, Berlin, pp 551–590

Katnam KK, Crocombe AD, Sugiman H, Khoramishad H, Ashcroft IA (2011) Int J Dam Mech 20:1217

Khoramishad H, Crocombe AD, Katnam K, Ashcroft IA (2010a) Int J Fatigue 32:1146

Khoramishad H, Crocombe AD, Katnam K, Ashcroft IA (2010b) Int J Adhes Adhes 32:1278

Khoramishad H, Crocombe AD, Katnam K, Ashcroft IA (2011) Eng Fract Mech 78:3212

Landes JD, Begley JA (1976) Mechanics of crack growth, ASTM STP 590. American Society for Testing and Materials, Philadelphia, pp 128–148

Levebvre DR, Dillard DA (1999) J Adhes 70:119

Little MSG (1999) Durability of structural adhesive joints. Ph.D. thesis, London, Imperial College of Science, Technology and Medicine

Manson SS (1954) Behaviour of materials under conditions of thermal stress. In: National Advisory Commission on aeronautics. Report 1170. Lewis Flight Propulsion Laboratory, Cleveland, pp 317–350

Miner MA (1945) J Appl Mech 12:64

Nisitani H, Nakamura K (1982) Trans Jpn Soc Mech Eng 48:990

Oinen A, Marquis G (2011) Eng Fract Mech 78:163

Palmgren A (1924) Z Ver Dtsch Ing 68:339

Paris PC, Gomez MP, Anderson WE (1961) Trend Eng 13:9

Pirondi A, Moroni F (2010) J Adhes 86:501

Quaresimin M, Ricotta M (2006) Comp Sci Technol 66:647

Rice JR (1968) J Appl Mech 35:379

Saxena A (1986) In: Underwood JH et al (eds) Fracture mechanics: seventeenth volume, ASTM STP 905. American Society for Testing and Materials, Philadelphia, pp 185–201

Schaff JR, Davidson BD (1997a) J Comp Mater 31:128

Schaff JR, Davidson BD (1997b) J Comp Mater 31:158

Shenoy V, Ashcroft IA, Critchlow GW, Crocombe AD, Abdel Wahab MM (2009a) Int J Adhes Adhes 29:361

Shenoy V, Ashcroft IA, Critchlow GW, Crocombe AD, Abdel Wahab MM (2009b) Int J Fatigue 31:820

Shenoy V, Ashcroft IA, Critchlow GW, Crocombe AD, Abdel Wahab MM (2009c) Int J Adhes Adhes 29:639

Shenoy V, Ashcroft IA, Critchlow GW, Crocombe AD (2010a) Int J Fatigue 32:1278

Shenoy V, Ashcroft IA, Critchlow GW, Crocombe AD (2010b) Eng Fract Mech 77:1073

Walander T, Eklind A, Carlberger T, Stigh U (2014) Proc Math Sci 3:829